ARTICLE IN PRESS

Tunnelling and Underground Space Technology xxx (2010) xxx–xxx

Contents lists available at ScienceDirect

Tunnelling and Underground Space Technology

journal homepage: www.elsevier.com/locate/tust

Analysis and optimization of ventilation systems for an underground transport interchange building under regular and emergency scenarios

Jerónimo Domingo [a], Rubén Barbero [a], Alfredo Iranzo [b,*], Daniel Cuadra [a], Jorge Servert [c], Marco Antonio Marcos [d]

[a] ANALISIS-DSC, C/Ntra, Señora de la Luz, 21, 28025 Madrid, Spain
[b] Thermal Engineering Group, Energy Engineering Department, University of Seville, Camino de los Descubrimientos, s/n. 41092 Seville, Spain
[c] TTC Trabajos Técnicos y Científicos, Plaza de Manolete, 2, 11-C, 28020 Madrid, Spain
[d] DICYP, Sierra de Cazorla, 1, Pta. SS, Oficina D, Las Matas, Las Rozas, 28230 Madrid, Spain

ARTICLE INFO

Article history:
Received 8 November 2009
Received in revised form 7 July 2010
Accepted 25 July 2010
Available online xxxx

Keywords:
Transport interchange building
Computational Fluid Dynamics
Ventilation
Fire simulation
Smoke control

ABSTRACT

The work and conclusions gained from the analysis of five new underground interchange buildings ongoing in Madrid, Spain, is presented. An additional study was performed for a typical two-level interchange building, and the methodology and results are presented in this paper.

First, different ventilation and air conditioning strategies have been analyzed. The main goal is to find the most efficient design in order to maintain pollutants concentration and temperatures below the designed values, at minimum investment and operation costs. Different strategies have been modelled and compared using a Computational Fluid Dynamics (CFD) code, taking into account the buses circulation and the different pollution and heat sources. The final solution developed is based on a physical separation between the island area and the dock area. Conclusions on the efficiency of the different design strategies and possible pitfalls are presented.

Secondly, different fire scenarios are analyzed. The main goal is to check whether the fire fighting measures planned, such as mechanical ventilation and a curtains system to define smoke sectors are able to cope with a fire emergency situation. A model for the bus fire has been developed, including heat release and smoke production. The main results presented are temperature fields, visibility and smoke concentration.

© 2010 Elsevier Ltd. All rights reserved.

1. Introduction

Easy, fast and convenient transport interchange is necessary to improve public transport. Due to the lack of space in large cities a solution currently being implemented is underground interchange building constructions, where each level is devoted to one mean of transport: metropolitan buses, city buses, long-range buses, subway and train.

A comprehensive design of such and similar buildings must take into account the air flow behaviour in different conditions. First, heating, ventilation and air conditioning design must ensure comfort conditions for passengers with minimum investment and operation costs. Secondly, ventilation under emergency conditions such as different fire scenarios must ensure a rapid evacuation and efficient smoke management.

Computational Fluid Dynamics (CFD) has proven to be a powerful tool for the prediction of air flow and related variables distribution, thus helping the design and evaluation of HVAC and fire emergency systems under a wide range of scenarios. Liu et al. (2009) analysed the characteristics of buoyancy driven flown in atrium buildings, and Stavrakakis et al. (2008) compared experimental measurements with CFD simulations of natural cross ventilation in buildings, with relatively well results. Kato et al. (1992) also reports numerical results with very well agreement with wind tunnel experiments for natural cross ventilation. Wong et al. (2006) also performed thermal field measurements and comfort surveys in a large building, addressing the effectiveness of mechanical ventilation systems by means of CFD. There have been attempts to integrate CFD with other simulation techniques such as multi-zone models, as in the work reported by Tan and Glicksman (2005) for natural ventilation prediction. Not only focus on design validation or evaluation, numerical simulation also constitutes a design tool for optimization, as demonstrated by Hangan et al. (2001) and Yuan and You (2007) for complex atriums and subway stations respectively.

Significant work on CFD simulation of emergency scenarios under fire and smoke has been done. Road or train tunnels have been analysed to address the critical ventilation values, as in the work of Van Maele and Merci (2008), Yang et al. (2006), Hwang

* Corresponding author. Tel.: +34 914614071; fax: +34 914628257.
E-mail address: aip@esi.us.es (A. Iranzo).

0886-7798/$ - see front matter © 2010 Elsevier Ltd. All rights reserved.
doi:10.1016/j.tust.2010.07.001

Please cite this article in press as: Domingo, J., et al. Analysis and optimization of ventilation systems for an underground transport interchange building under regular and emergency scenarios. Tunnel. Underg. Space Technol. (2010), doi:10.1016/j.tust.2010.07.001

Nomenclature

g	gravity acceleration (m/s^2)
h	enthalpy (J/kg)
k	turbulent kinetic energy (m^2/s^2)
p	static pressure (Pa)
S_M	momentum source term (kg/m^{2}s^2)
T	temperature (K)
t	time (s)
$\overline{U}$	velocity vector (m/s)
u, v, w	velocities in x, y, z (m/s)
x, y, z	spatial directions (m)

Greek letters

ε	turbulence eddy dissipation (m^2/s^3)
μ	dynamic viscosity (Pa s)
ρ	fluid density (kg/m^3)
ω	turbulence eddy frequency (1/s)

and Edwards (2005), Gao et al. (2004) and Galdo-Vega et al. (2008), who also reports a validation of numerical simulation results against experimental measurements.

Available computing power was limiting the application of CFD techniques to small buildings in the past, but nowadays it is possible to model larger buildings with a relative high accuracy. The use of three-dimensional modelling tools such us CFD enables the improvement of the design, construction, operation and maintenance of underground buildings, allowing to plan more cost-effective techniques at all stages of development, and for a quantitative analysis of the results, the same ventilation parameters developed for experimental measurements (ventilation efficiency, removal efficiency and other ventilation parameters as stated in Chan and Chow (2004)) can also be considered.

2. Numerical methods

The CFD simulations are based on the resolution of the Navier–Stokes equations. The numerical model resolves the three velocity components and mass conservation equations linked via a pressure–velocity coupling algorithm. Energy for the temperature field resolution is resolved as well. Scalars such as relative humidity (RH) and pollutant concentrations (CO, NO_x) are computed and solved as a transport equation in the domain. This is included in the ventilation analysis, whereas smoke concentration and radiation intensity are resolved for the fire scenarios. Therefore, the set of equations solved are the three-dimensional Navier–Stokes (N–S) equations in their steady-state conservation form. The transport equations are the general form of conservation law for the airflow variable ϕ:

$$\frac{\partial}{\partial t}(\rho\Phi) + div(\rho\vec{V}\Phi) = div[\Gamma_\Phi grad(\Phi)] + S_\Phi \tag{1}$$

where ρ is density, Γ_ϕ and S_ϕ are the diffusivity and the source term, respectively. $\vec{V}$ is the velocity of the air flow expressed in terms of the components u, v, w along the x, y, z coordinates. The airflow variables ϕ are the velocity components u, v, w, enthalpy h, turbulent kinetic energy k, and dissipation rate of kinetic energy ε and pollutants and smoke concentration. The continuity equation derived from the general N–S equation reads:

$$\frac{\partial p}{\partial t} + \nabla \cdot (\rho\overline{U}) = 0 \tag{2}$$

And the momentum conservation equations (in x, y, z directions) read:

$$\frac{\partial p\overline{U}}{\partial t} + \nabla \cdot (\rho\overline{U} \otimes \overline{U}) = -\nabla p + \nabla \cdot \tau + s_M \tag{3}$$

where τ is the stress tensor.

The simulations performed in the ventilation and fire simulations corresponded to steady-state scenarios, so that the transient term in Eqs. ((1)–(3)) were not considered.

Flow is dominated mainly by mechanical ventilation and buoyancy especially near the fire. Given the buoyant nature of the flow due to the heat release (either by thermal loads such as bus gas emissions in the ventilation analysis or combustion in the fire analysis), a source term is included in the momentum equation as follows:

$$S_{M,\text{buoyancy}} = (\rho - \rho_{\text{ref}})g \tag{4}$$

where ρ is the fluid local density and ρ_{ref} is a reference density.

Turbulence aids promoting the diffusion rate of mass, momentum and heat. In all cases turbulence was modelled via the Shear Stress Transport (SST) model (Menter, 1994) with automatic wall functions. It is a two-equation eddy viscosity model that accounts for the transport of the shear stress and gives highly accurate predictions of the turbulence phenomena. It consists of a blending of the k–ε model in the core of the fluid and the k–ω model in the near-wall region. The blending function is based on the distance to the nearest wall and on the flow variables.

The CFD solver used for the simulations was the commercial CFD code ANSYS CFX (ANSYS Inc., 2006). The Navier–Stokes conservation equations described above are discretized using an element-based finite volume method (Raw, 1994). The discretization is fully conservative and time-implicit. The conservation equations are integrated over each control volume, where volume integrals are converted to surface integrals using Gauss' divergence theorem, and surface fluxes are evaluated in exactly the same manner for the two control volumes adjacent to an integration point. The advection scheme used to evaluate the variables is extremely important for the solution accuracy. A bounded high-resolution scheme is used as described by Barth and Jesperson (1989). The mass flows must be discretized in a careful manner to avoid pressure–velocity decoupling. This is performed by generalizing the interpolation scheme proposed by Rhie and Chow (1982). The solver solution strategy is based on a coupled solver, which solves the hydrodynamic equations (for u, v, w, p) as a single system. The linear system of equations is solved using a coupled algebraic multigrid technique (Raw, 1996).

The mesh contains 2.6 million tetrahedral elements, with an average cell size of 25 cm. The appropriate mesh refinement was performed near the walls by generating a set of prism layers, and near the fire area by locally refining the mesh element size.

3. Ventilation analysis

One of the questions in the design of transport interchange building air conditioning and ventilation systems is whether to use slot diffusers, jet nozzles or swirl diffusers for forced air intake. Different designers are prompt to defend one of them (Hama et al., 1974) but a scientific demonstration of their performance on real operation is not available in the literature.

Please cite this article in press as: Domingo, J., et al. Analysis and optimization of ventilation systems for an underground transport interchange building under regular and emergency scenarios. Tunnel. Underg. Space Technol. (2010), doi:10.1016/j.tust.2010.07.001

It is one aim of the present paper to analyse this subject. For this purpose, the geometry of a generic interchange building has been developed, containing various air intake systems such as slot diffusers, jet nozzles and rotational diffusers. The geometry is shown on Fig. 1 for slot diffusers. The underground building has two levels, communicated by ramps. In the centre of each level a closed island area with automatic doors is keeping waiting passengers away from lower comfort conditions in the dock area. Slot diffusers are used for air exhaust for all cases. For each scenario a different air intake system will be activated. The total volume of the interchanger building is ca. 56.000 m^3, with general dimensions of 120 m in length and 65 m in width. Similar studies can be found in the work of Papakonstantinou et al. (2003) although only CO was considered as pollutant and different ventilations designs were not considered.

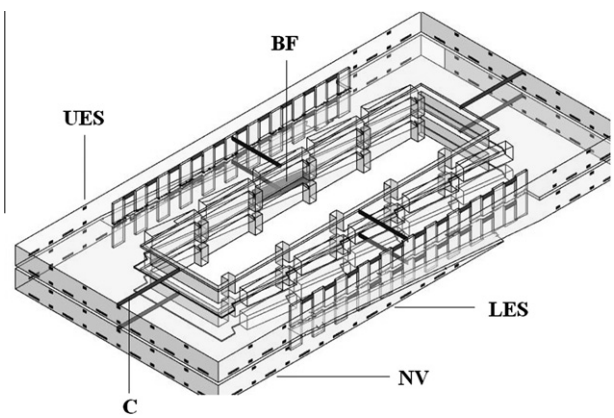

Fig. 1. Transport interchange building showing walls, upper (UES) and lower (LES) exhaust slots and natural ventilation slot diffusers (NV), dock area, structural ramp supporting columns, and buses. The bus in fire is located in the lower level (BF). Curtains (C) can be appended to or deactivated from the simulation.

3.1. Operating conditions for ventilation modelling

For the ventilation system analysis the air intake is set to eight air changes per hour (ACH), which is an average value for normal operation that may be increased at certain cases such as rush hours or fires. The location in height of both air intake and exhaust has been divided into two sections according to the authors former research work: one at knee height in order to drag pollutants from punctual sources like bus gas exhausts, and a second one close to ceiling height, where heat and pollutants tend to accumulate. Previous calculations lead to an optimal flow distribution: 70% in the upper section and 30% in the bottom section, both for air intake and exhaust. The air intake temperature is 28 °C and 80% relative humidity, due to adiabatic cooling for Madrid summer conditions, and pollutant concentration in the air intake is assumed to be zero.

The main sources of pollutants and heat are the buses. The buses are divided into three different groups (a) idle buses, with no pollutant emission but engine and breaks are still at high temperatures and remain emitting heat, (b) parked buses before departure, where heat is emitted by the engine and pollutants exiting the exhaust duct end, and (c) circulating, where emissions are initially concentrated at the exhaust duct and lately diffused by the bus movement. This is modelled as a source of moment and turbulence kinetic energy. The values of the different pollutant emissions are available from ASHRAE, HVAC applications Handbook (2003) and the PIARC Technical Report (2004). However, the values specified in the EURO IV (Directive 98/69/EC of the European Parliament) were used in the simulation given its local application in Spain. The pollutants considered are thus CO and NO_x, being the values of emission 2.36e–06 kg/s and 5.0e–06 kg/s, respectively, for idling buses, and 3.0e–06 kg/s and 6.4e–06 kg/s, respectively, for circulating buses (10 km/h). The heat released according to André et al. (1994) from each bus is 42 kW/bus and from the ceiling illumination, 10 W/m^2.

The long-range bus level (−1) has a lower bus density than the city bus level (−2). Bus circulation in −2 level is modelled via a source of momentum proportional to the relative speed of air to

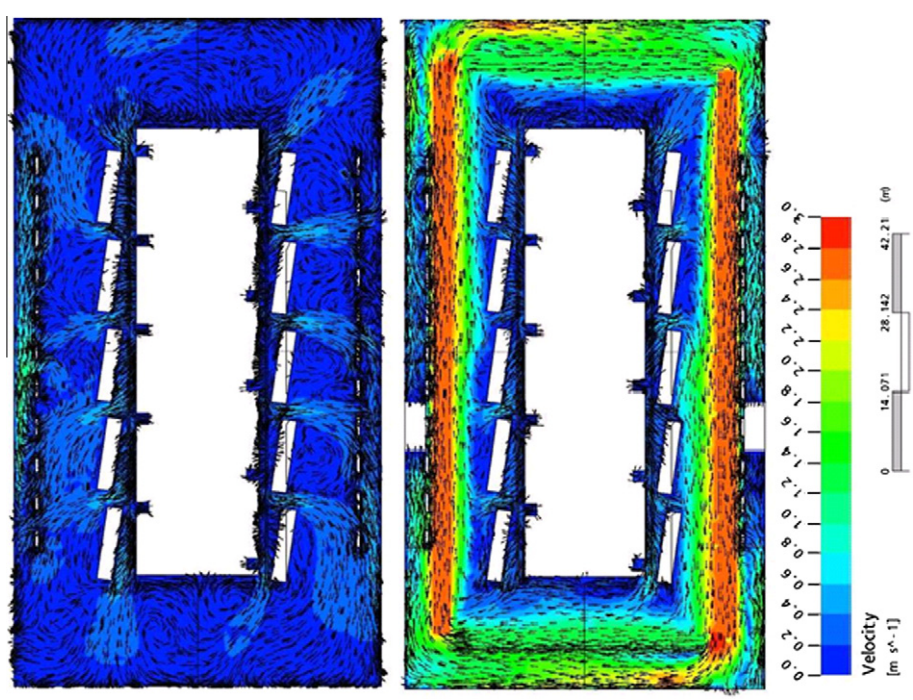

Fig. 2. Velocity distributions with slot diffusers at height 1.5 m: upper level (left), lower level (right).

Please cite this article in press as: Domingo, J., et al. Analysis and optimization of ventilation systems for an underground transport interchange building under regular and emergency scenarios. Tunnel. Underg. Space Technol. (2010), doi:10.1016/j.tust.2010.07.001

the bus, according to the model of Silva and Viegas (1994). The bus velocity is 10 km/h in the building long sides and 5 km/h in the short ones. The momentum source was included in a 3D subdomain located all along the buses road (see larger velocity areas in Fig. 2, right). Local turbulence generation is also included by defining a turbulent kinetic energy source in the same subdomain, as well as the corresponding heat and pollutants sources. Therefore, the interaction effects between air intake streams and bus movement is considered, as the local 3D flow field governed by the Navier–Stokes equations (Eqs. (2) and (3)) is influenced by both effects in the confluence of air intake streams and buses road.

Three different scenarios have been resolved where the only difference is the upper air intake device:

- *Case 1A:* long slot diffuser, modelled with a normal velocity inlet.
- *Case 1B:* jet nozzles, modelled with a normal velocity inlet.
- *Case 1C:* swirl diffuser, that introduces air with a rotational or swirl component according to the technical specifications from a worldwide known manufacturer.

3.2. Results for the ventilation scenarios

3.2.1. Case 1A: slot diffuser

The first scenario corresponds to case 1A with a slot diffuser-type air intake. The velocity field is shown in Fig. 2 for the upper and lower levels. Buses are circulating in the lower level, and in Fig. 2 can be observed the main air flow pattern where the buses produce a screen effect that forces the flow to accelerate in its way out through the spaces between them. The transversal section of the air flow from the intakes to the exhaust is also important. Along this way, air will drag pollutants and heat, and the efficiency of this process during the path determines the efficiency of the ventilation system of the building.

Regarding air quality and comfort, Fig. 3A shows the temperature field in −1 level and −2 levels. In −1 level temperature ranges from 28 °C (bottom of the figure) to 30 °C (top of the figure), despite the building symmetrical design. This is the result of the warmer air of level −2 arriving to the level −1 through the ramps.

Fig. 3A shows that the clockwise movement of the circulating buses in −2 level produces a drag or piston effect on the air. In the upper zone of the picture the pollutants and heat concentrates. The connection through ramps causes that this situation on level −2 is also affecting level −1.

The results for NO_x distribution in parts per million (hereafter ppm), shows a similar effect. Clean ventilation air is assumed to contain no NO_x. For level −2, Fig. 3B shows the two pollutant sources, circulating and stopped buses, and the drag effect of the first ones on the whole level. Fig. 3C shows the RH filed in level −1 and −2, respectively.

3.2.2. Case 1B: jet nozzles

The results for case 1B with jet nozzles are presented next. Jet nozzles are located on the sides of the dock ceiling. Due to the high speed air flow inlet through the jet nozzles there are wide zones surrounding the jet nozzles with high air velocity. A flow circula-

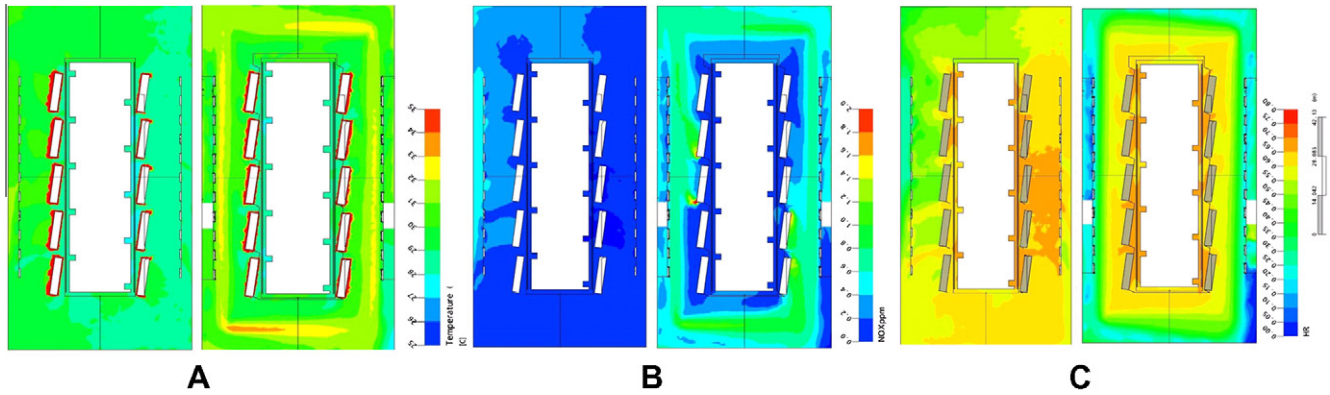

Fig. 3. Distributions of comfort variables at height 1.5 m with slot diffusers: upper level (left), lower level (right). (A) Temperature distribution, (B) NO_x distribution, (C) relative humidity distribution.

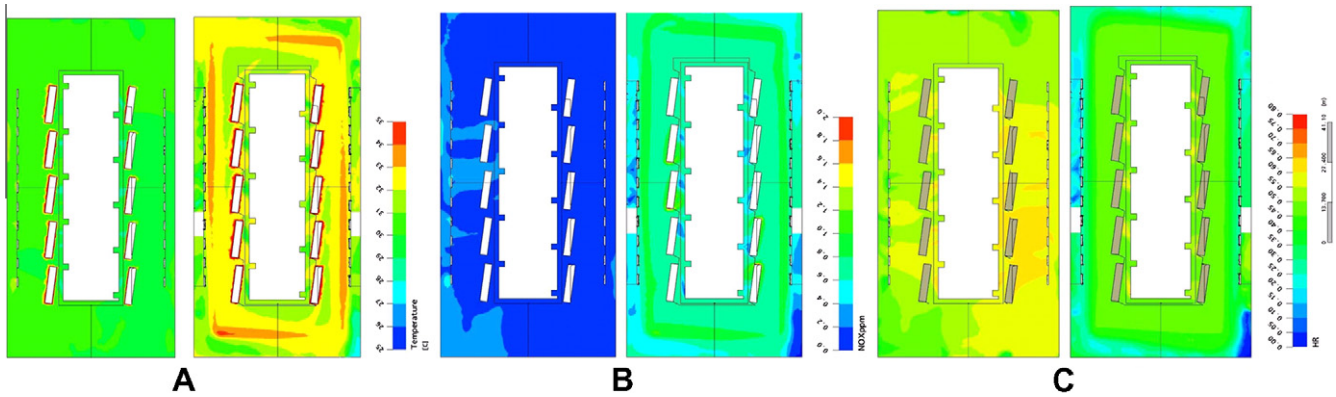

Fig. 4. Distributions of comfort variables at height 1.5 m with jet nozzles: upper level (left), lower level (right). (A) Temperature distribution, (B) NO_x distribution, (C) relative humidity distribution.

Please cite this article in press as: Domingo, J., et al. Analysis and optimization of ventilation systems for an underground transport interchange building under regular and emergency scenarios. Tunnel. Underg. Space Technol. (2010), doi:10.1016/j.tust.2010.07.001

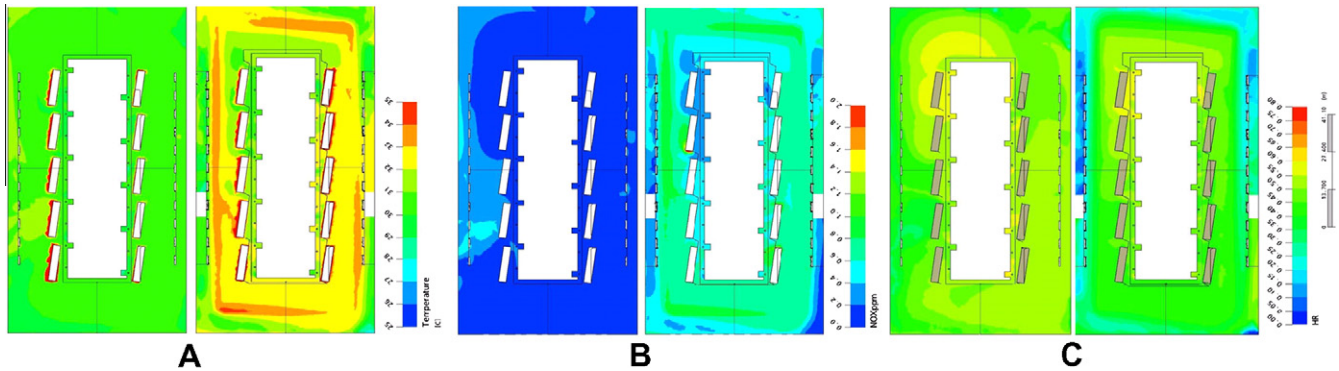

Fig. 5. Distributions of comfort variables at height 1.5 m with swirl diffusers: upper level (left), lower level (right). (A) Temperature distribution, (B) NO_x distribution, (C) relative humidity distribution.

tion is produced, where the air flows along the ceiling from the dock area to the external walls, falls down and turns back towards the island. The air at the centre remains with low speeds.

Temperature fields are shown in Fig. 4A for level −1 and level −2. Temperature field appears to present higher values even in the upper level than in the scenario with slot diffuser inlets, as the whole level is above a temperature of 30 °C.

The temperature in the lower level shown at Fig. 4A is generally higher than in the case with slot diffuser-type inlet. The distribution remains the same but the averaged temperature is about 2 °C higher reaching 30 °C. This effect increases up to an excess of 5 °C in the passenger waiting zone, from 27 °C in the slot diffuser case to 32 °C for the jet nozzle case.

The NO_x distribution in level −1 can be observed in Fig. 4B. NO_x concentrates on the upper side of the picture, where due to buses circulating clockwise pollutants concentrate. Comparing to the slot diffuser case, it is observed that high concentrations are also located closer to the outer walls, but passenger zone presents in general slightly higher concentrations. Slot diffuser-type inlets show therefore better performance in terms of pollutant concentration. In the lower level, jet nozzles produce a quite even NO_x concentration distribution, in the range 0.8–1.0 ppm, except for the corners. The slot diffuser inlets produce a less even distribution, from 0.0–1.2 ppm, where the cleaner zones are precisely the passenger areas. Therefore, slot diffuser-type inlets are a much more efficient method for the purpose of passenger comfort.

The relative humidity distributions (Fig. 4C) appear also to be more even in the scenario with jet nozzles than with slot diffuser, in a range of 40–65% for the upper level and 35–50% in the lower level. In the proximities of the outer walls RH falls to 15–30%. For the slot diffuser case, due to the higher "moving outwards" effect, the distribution is stratified vertically from island to the outer walls, reaching in the passenger zones RH values up to 65–75%.

Therefore, it can be asserted that slot diffusers produce a larger drag effect on the flow and a more stratified flow field, while jet nozzles produce a more significant mixing effect, yielding a more even distributed variables field. The selection of the optimal system will depend on whether a certain zone with better comfort is required, or more a wide and averaged comfortable atmosphere is required.

Table 1
Results summary of the three air intake systems analysed.

	Temperature (°C)	NO_x (ppm)	RH (%)
Slot diffuser	28.5	0.07	33
Jet nozzle	31.4	0.59	28
Swirl diffuser	31.5	0.57	26

3.2.3. Case 1C: swirl diffuser

The results for case 1C with swirl diffusers are presented next. The velocity field is more complex and generally higher velocities in the passenger area can be observed. A high speed area is formed above the stopped buses avoiding the pollutants and heat to enter from the circulating zone to the passenger zone.

The temperature field (Fig. 5A) in the upper level is quite even, although a bit less than in the jet nozzle case, being the range around 31 °C with small zones at 32 °C. For the lower level the temperatures are generally the highest of the cases analysed, reaching 33–35 °C in the bus circulating zone and about 31–32 °C in passenger zone. Again the upper figure part concentrates larger hotter areas.

The NO_x distributions shown in Fig. 5B are quite similar to the previous cases, but passenger zones remain completely clean in the upper level. The lower level presents a quite even distribution, but not as much as for the jet nozzle case with local zones on the passenger area remaining quite clean. The general concentration values are slightly lower than in the jet nozzle case, being in the range 0.6–0.8 ppm.

Finally, Fig. 5C shows the RH distributions. On the upper level the value range and distribution are similar to the scenario with jet nozzles. For the lower level the circulating buses produce a screen effect leading to a stratified HR pattern from the dock area to outer walls.

Table 1 summarizes averaged values of temperature, pollutant concentrations and relative humidity in the passenger area. The volume average has been calculated in a domain covering the passenger zone from the island dock wall to the buses, and in a height range from 0.5 to 2 m. Only the lower level is considered as the upper level presents low heat and pollutant loads.

4. Fire analysis

A fire scenario has been modelled and analysed in order to asses the emergency operation performance of the interchange transport facility. The geometry of the building is shown in Fig. 1. The underground building has two levels, communicated by ramps. In a basic scenario the fire outbreaks in a bus stopped in the lower level.

Different fire protection strategies have been analysed for the building. The ceiling area can be divided into sectors separated by short curtains to stop the smoke propagation and facilitate its extraction. Two different forced smoke extraction flow rates are analysed: the base case has an exhaust flow equal to eight air changes per hour (ACH), which correspond to the standard ventilation needs, and for a different scenario, a 50% increase equal to 12 ACH is analyzed. Hence, three cases are considered:

– *Case 2A:* with curtains and 50% increased exhaust flow.
– *Case 2B:* without curtains and basic exhaust flow.
– *Case 2C:* with curtains and basic exhaust flow, corresponding to the standard ventilation operation.

Curtains have the purpose of creating divided smoke pools under the ceiling where the smoke reaches a higher concentration and exhausting system can therefore be more efficient, extracting more smoke and heat with the same exhausted flow. Hence, the inclusion of curtains delays the spreading of smoke to other zones and concentrates smoke in the fire out breaking zone, which should be evacuated immediately. It is therefore desirable that the exhausting slot diffusers are placed above the curtain lower edges to assure curtain efficiency. Exhausting slot diffusers on ceilings instead of on walls should be considered. Also, the curtain height should be maximized attending to the buses heights. However, the local regulation allows only for curtains less than 60 m in length and ceiling sectors less than 2000 m^2. The curtain depth considered in this case was 0.50 m. Smoke extraction is carried out only in the sector where the fire has been detected in order to prevent smoke suction to other areas.

The fire and smoke propagation dynamics have been modelled for 10 min following the rate defined in PIARC (1999), thus a transient model is used.

In Fig. 1 the burning bus is represented as a grey parallelepiped, the exhausting slot diffusers in black (squares near the ceiling), the natural ventilation slot diffusers are modelled as rectangles near the level, and the curtains are modelled as perpendicular walls to the ceiling. Natural ventilation slot diffusers assure an oxygen rich fire, avoiding additional toxic compounds and blazes, which are more dangerous for passengers.

4.1. Operating conditions for fire modelling

The heat release rate has been modelled following PIARC Montreal report (1999), where the maximum heat release for a standard bus is 20 MW after 12 min. The gas products mass flow has been calculated based on the hypothesis of complete combustion, with a combustion heat equal to 12 MW/KgO_2, and a fuel with a hydrogen/carbon H/C ratio of 1.5.

The heat of combustion and fuel characterisation has been estimated from typical bus materials according to the Fires in Mass Transit Vehicles report from National Research Council (1991). The combustion heat has been estimated according to the Handbook of Fire Protection Engineering (1995). Heat release has been referred to O_2 mass burnt due to its lower variation with fuel composition. Products are computed by adding scalar variables, where the concentrations are evaluated supposing complete reaction as described in the work by Hubbard and Tien (1978). Radiation heat fluxes have also been evaluated, taking soot as the main contribution in the absorption coefficient evaluation according to Felske and Tien (1975, 1977) and Yuen and Tien (1977).

Considering a bus fire scenario with a heat release of 20 MW, and a standard facility occupation, it is assumed that the fire alarm is manually activated either by the passengers or the facility personnel, immediately after the fire onset. Therefore it is assumed that the egression starts immediately after the fire onset. After the alarm activation, the time needed by the ventilation system to change from regular operation to emergency operation is 1 min.

4.2. Results for the fire scenarios

The temperature, heat radiated, visibility and toxic gases concentration are the most important variables to be analysed, due to their effect on human health and evacuation procedures. Graphical results shown in this section are presented in planes at 1.5 m height, assuming this as the typical human head location. To evaluate the fire effects, the situation has been analyzed every minute. The most relevant results are shown in this section. There are other effects related to bus fires in these types of buildings to be analyzed: radiation, fire toxic emission concentration, sprinkler effects, temperatures upon structures in order to estimate thermal fatigue and possible structure collapse, and the use of PROBIT analysis for the estimation of human mortality probability.

4.2.1. Results with curtains and with increment of exhaust flow rate

A comprehensive analysis of the situation at 10 min after the fire initiation has been performed. Summarizing the results, smoke concentration after 10 min shows that the upper level is completely filled up with smoke thus hindering visibility, which presents values in the range of 0–10 m (non-admissible). Hot smoke has entered into the upper level through the ramps. The lower level has a smoke layer close to the ceiling, leaving a smoke free height similar to human height. In most of the lower level, temperature is within a reasonable range between 40 and 50 °C. In the upper level the temperature is above 60 °C, considered as the safe limit value, reaching 70 °C or higher. Hence, at this time, upper level should have been completely evacuated. In the lower level visibility is between 10 and 20 m (admissible). Hence, at 10 min the situation is acceptable on level −2 and unacceptable in level −1.

Fig. 6A shows a longitudinal section of the temperature field, where the stratification is clearly observed. Highest temperatures are located at ceiling level, ramps and close areas to the burning bus.

Additional simulations have been performed using the evacuation software LEGION (Legion International Ltd., Still (2000), Zhou et al. (2010)). The results show that 6 min is the time needed to successfully evacuate the building, and therefore the situation at

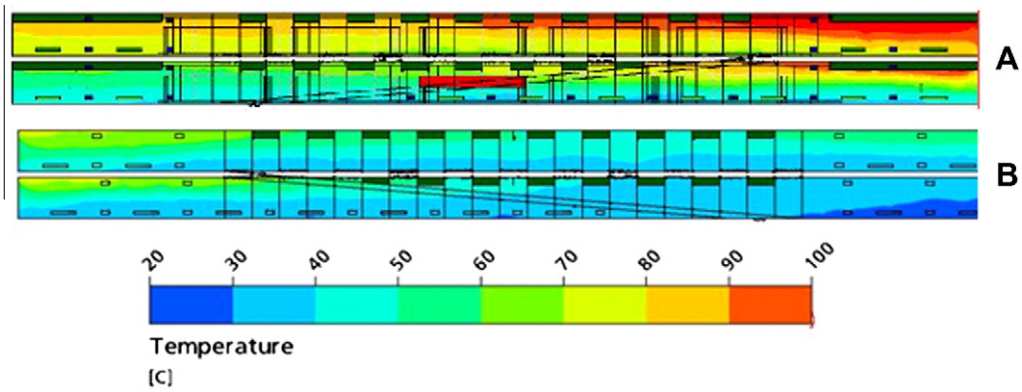

Fig. 6. Distribution of temperature field showing the vertical stratification in case 2A. (A) Time = 10 min, (B) time = 6 min.

Please cite this article in press as: Domingo, J., et al. Analysis and optimization of ventilation systems for an underground transport interchange building under regular and emergency scenarios. Tunnel. Underg. Space Technol. (2010), doi:10.1016/j.tust.2010.07.001

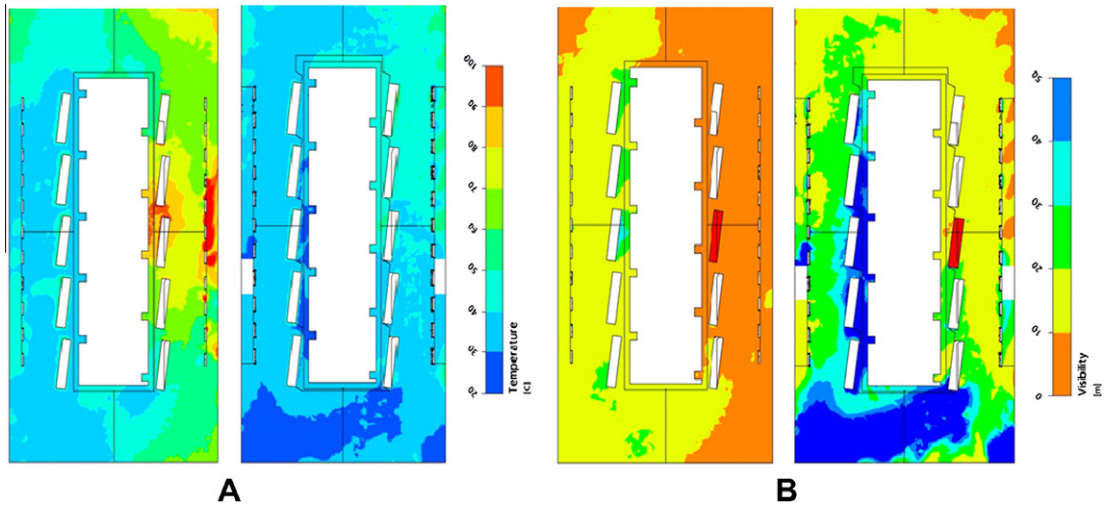

Fig. 7. Distribution of fire safety variables at height 1.5 m in case 2A in upper level (left), lower level (right). (A) Temperature, (B) visibility. Time = 6 min.

6 min will be analyzed here. As it was discussed in Section 4.1, it is assumed that the egression starts immediately after the fire onset. After the alarm activation, the time needed by the ventilation system to change from regular operation to emergency operation is 1 min.

The results for time 6 min show that the upper level temperatures (Fig. 7A) present high values on the surroundings of the ramp closest to the bus fire reaching 60 °C or higher. The rest of the level remains at about 40 °C.

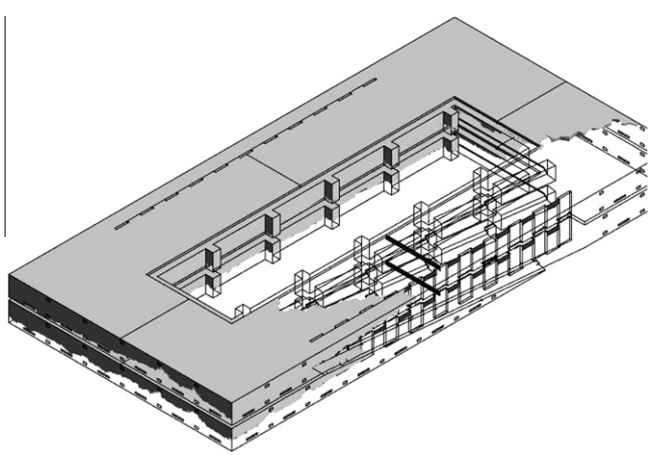

Fig. 8. Volume occupied by dense smoke, time = 6 min, case 2A.

The lower level (Fig. 7A) presents several zones: one zone of low temperature, screened from the fire by the island. Other zone is that near the fire towards the ramp, where the temperature reaches 50 °C, slightly below risk limit. Along the ramp, there are some spots with temperature 60 °C. Nevertheless, almost the entire lower level remains under risk limit temperature.

The temperature field in a section of the building after 6 min can be seen in Fig. 6B. Most of the building remains at acceptable temperatures.

The visibility in the building at 6 min is shown in Fig. 7B. On the upper level, smoke occupies a volume only near the ramp. On the lower level, only the fire surroundings around 20 m have a medium visibility, the rest has an acceptable and even good visibility, allowing the passenger evacuation. Passengers will have more than 6 min to evacuate with the only condition of avoiding the bus area.

Fig. 8 shows the volume occupied by dense smoke after 6 min. The smoke is stratified and concentrates above person height in most areas. Therefore, at 6 min the situation is safe for human beings in terms of visibility.

4.2.2. Results without curtains and without increment of exhaust flow rate

The following case is equal to the first one but putting away the curtains, in order to check their effect by checking the differences between the two cases.

The visibility on the 10th minute in both levels remains similar to the base case. The volume of dense smoke in the minute 10th is also similar to the base case.

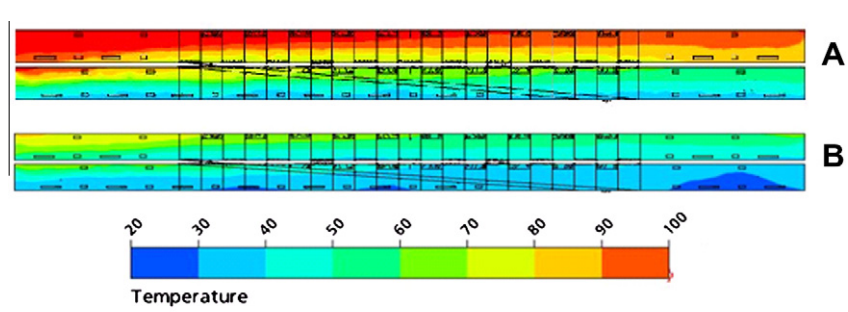

Fig. 9. Distribution of temperature field showing the vertical stratification in case 2B. (A) Time = 10 min, (B) time = 6 min.

Please cite this article in press as: Domingo, J., et al. Analysis and optimization of ventilation systems for an underground transport interchange building under regular and emergency scenarios. Tunnel. Underg. Space Technol. (2010), doi:10.1016/j.tust.2010.07.001

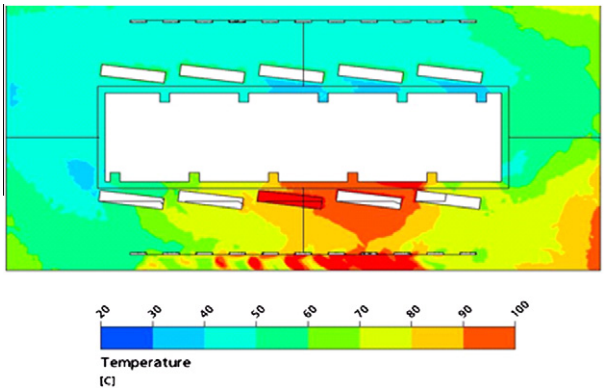

Fig. 10. Temperature field in upper level, time = 6 min, case 2B.

Regions with temperature values in the upper level over 100 °C are larger than in the case with curtains, while for the lower level the changes are minor.

This situation can be observed better in a longitudinal section as shown in Fig. 9A. Compared to case 2A shown in Fig. 6A, the height of high temperature is much lower in the upper level while there are no clear differences in the lower one. This means that in the previous case 2A much of the heat was stopped by the curtains while the exhausting flow took it away avoiding the free movement to the upper level, which loads it with higher temperatures at lower height. Then curtain installation improves the situation in upper level without making worse the lower one.

The results for the sixth minute are now presented. Compared to the base case the temperatures on the upper level are quite higher in the present case (Fig. 10) than in case 2A. In the lower level the difference is very small. In the curtain and incremented exhaust rate case the heat in the lower level was stopped by the curtains. This produced a high smoke stratification and the high exhausting rate extracted efficiently the smoke, remaining the level at acceptable temperatures. This is also observed in Fig. 9B for a cross section. In the present case the unstopped heat flows to the upper level. This makes that in lower level the differences are small but in the upper the situation is worse if curtains are not installed. This asserts the efficiency of curtains for the short and medium fire development time.

The visibility is shown in Fig. 11, and dense smoke in Fig. 12. Compared to case 2A the visibility is now reduced in the upper level. In the lower level is slightly better. Therefore, curtains certainly improve the situation also in terms of visibility, but not as much as in the case of temperatures.

4.2.3. Results with curtains and without increment of the exhaust flow rate

The temperature is very similar to the case without curtains at minute 10th at the upper level. But, as can be seen in Fig. 13, the temperature is higher at the lower level, reaching temperatures over 100 °C.

The visibility fields are quite similar compared to both former cases on the 10th minute. This means that counter measures permits larger times to passenger evacuation, but with large fires the final situation becomes unsafe in any case.

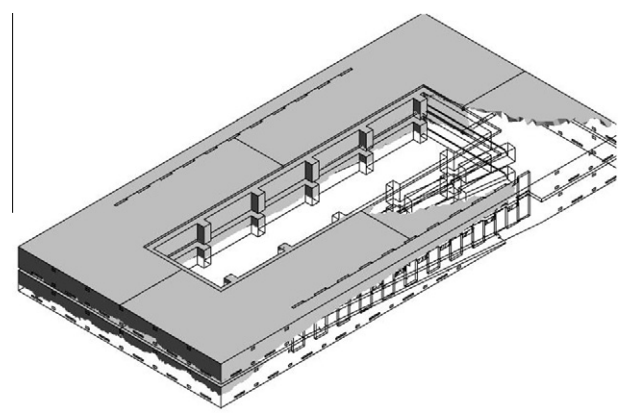

Fig. 12. Volume of dense smoke, time = 6 min, case 2B.

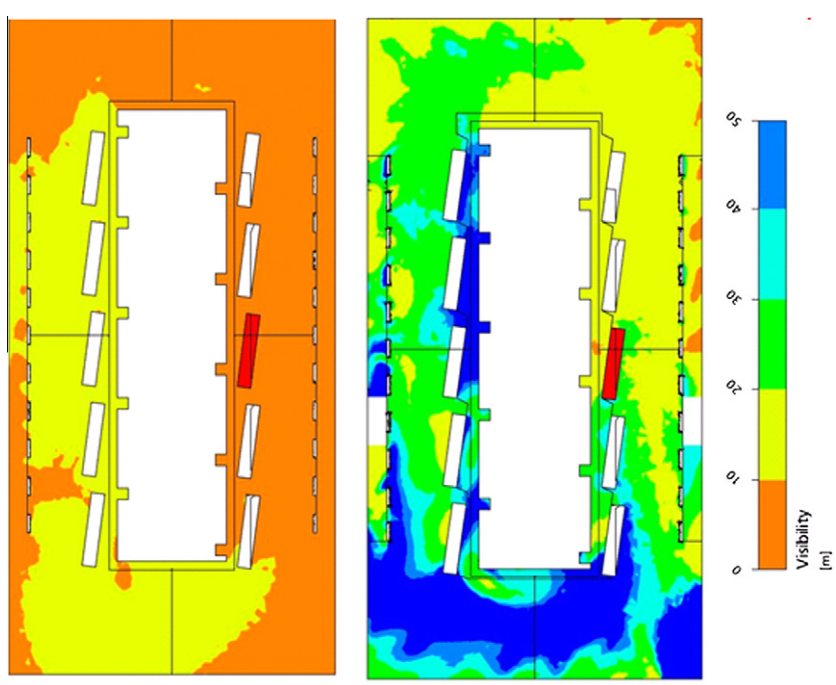

Fig. 11. Visibility field in upper level (left), lower level (right). Time = 6 min, case 2B.

Please cite this article in press as: Domingo, J., et al. Analysis and optimization of ventilation systems for an underground transport interchange building under regular and emergency scenarios. Tunnel. Underg. Space Technol. (2010), doi:10.1016/j.tust.2010.07.001

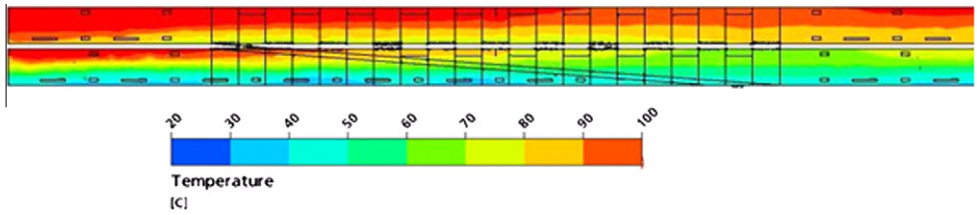

Fig. 13. Temperature profile, time = 10 min, case 2C.

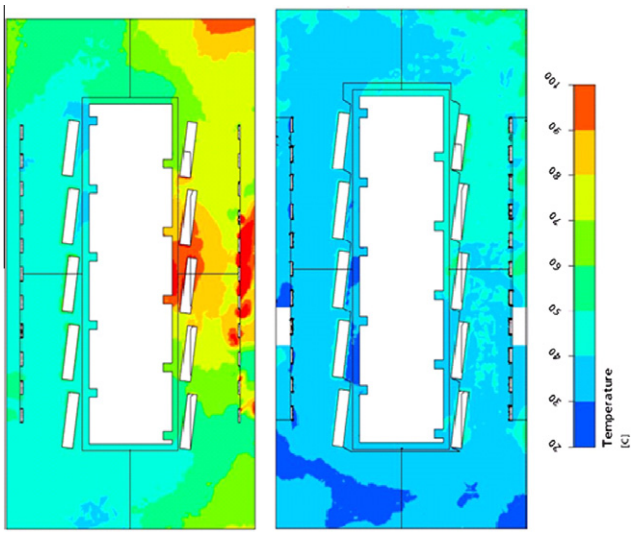

Fig. 14. Temperature field in upper level (left), lower level (right). Time = 6 min, case 2C.

Finally, for the sixth minute, the temperature in the upper level (Fig. 14) is lower than in the case 2B without curtains. The curtains are stopping the smoke in the lower level and the reduced exhausting flow is clearly not able to extract smoke enough.

Visibility shows the same pattern as temperature in the sixth minute. The situation in the lower level is slightly worse than in case 2B.

5. Summary and conclusions

Different ventilation and fire scenarios for an underground transport interchange building have been simulated by means of Computational Fluid Dynamics. This has been shown to be a powerful tool for the assessment of both passenger comfort and emergency operation performance. Based on the results, a complete set of guidelines for the building systems operation both in normal and emergency scenarios can be derived. The performance of different air intake and smoke countermeasure designs has also been shown.

Particular conclusions for each analysis are summarized below.

5.1. Conclusions for the ventilation analysis

(i) The transport interchange building performance has been simulated for different air intake devices: slot diffusers, jet nozzles and rotational diffusors. Results for two different levels with low and high bus densities have been shown.

(ii) The importance of 3D effects has also been discussed, where the circulation direction of the buses produces a drag effect on the surrounding air. Therefore it is necessary the simulation of the whole building, as partial or 2D simulations would miss important information. The role of stopped buses on the formation of a screen effect has also been discussed, and it has been observed that the situation on each level has an influence on other levels.

(iii) As a concluding remark, the slot diffuser-type air intake produces the larger heat and pollutants drag to the exhaust zones and therefore performs better. The jet nozzle solution produces the highest mixing solution, and the rotational solution results in an intermediate solution.

5.2. Conclusions for the fire analysis

(i) The simulation of a transport interchange building has been done for a range of fire and smoke countermeasures. It has been shown that there is a need for the simulation of the whole building, given the 3D effects, ramps and islands effects, and the coupling between the different levels and fire fighting countermeasures.

(ii) There are different possible countermeasures: curtains attending to their number and position, doors in ramps, sprinklers, etc. Curtains have the purpose of creating a smoke pools under the ceiling in which the smoke reaches a higher concentration and exhausting system can be more efficient extracting more smoke and heat with the same exhausted flow. Therefore, it is desirable that the exhausting slot diffusers are placed above the curtain lower edges to assure curtain efficiency. Exhausting slot diffusers on ceilings instead of on walls should be considered. Also, the curtain height should be maximized.

(iii) Another conclusion is that the exhausting system should be designed for at least a 50% higher capacity than the normal ventilation performance.

(iv) The central isolated island is a good safety measure, the evacuation time required by passengers to leave the dangerous area is now shorter as a safe place inside the island is closer, and it also produces a screen effect upon the fire, making the opposite side to burning bus a safe zone for evacuation.

References

André, J.C.S., Conceição, E.Z.E., Silva, M.C.G., Viegas, D.X., 1994. Integral simulation of air conditioning in passenger buses. In: Proceedings of the 4th International Conference on Air Distribution in Rooms – RoomVenť94.

ANSYS CFX Documentation, 1996–2006 ANSYS Europe, Ltd.

ASHRAE HVAC Applications Handbook, 2003. (SI Edition) – ISBN 1931862230.

Barth, T.J., Jesperson, D.C., 1989. The Design and Application of Upwind Schemes on Unstructured Meshes. AIAA Paper 89, 0366.

Chan, M.Y., Chow, W.K., 2004. Car park ventilation system: performance evaluation. Build. Environ. 39 (6), 635–643.

Felske, J.D., Tien, C.L., 1975. Wide band characterization of the total band absorptance of overlapping infrared gas bands. Combust. Sci. Technol. 11, 111–117.

Please cite this article in press as: Domingo, J., et al. Analysis and optimization of ventilation systems for an underground transport interchange building under regular and emergency scenarios. Tunnel. Underg. Space Technol. (2010), doi:10.1016/j.tust.2010.07.001

Felske, J.D., Tien, C.L., 1977. The use of the milne-eddington absorption coefficient for radiative heat transfer in combustion systems. J. Heat Trans. 99, 458.

Galdo-Vega, M., Argüelles-Díaz, K.M., Fernández-Oro, J.M., Ballesteros-Tajadura, R., Santolaria-Morros, C., 2008. Numerical 3D simulation of a longitudinal ventilation system: memorial tunnel case. Tunn. Undergr. Sp. Tech. 23 (5), 539–551.

Gao, P.Z., Liu, S.L., Chow, W.K., Fong, N.K., 2004. Large eddy simulations for studying tunnel smoke ventilation. Tunn. Undergr. Sp. Tech. 19 (6), 577–586.

Hama, G.M., Frederick, W.G., Monteith, H.G., 1974. How to design ventilation systems for underground garages. Air Engineering. Study by the Detroit Bureau of Industrial Hygiene, Detroit.

Hangan, H., McKenty, F., Gravel, L., Camarero, R., 2001. Case study: Numerical simulations for comfort assessment and optimization of the ventilation design for complex atriums. J. Wind Eng. Ind. Aerod. 89 (11–12), 1031–1045.

Hubbard, G.L., Tien, C.L., 1978. Infrared mean absorption coefficients of luminous flames and smoke. J. Heat Trans. 100–235.

Hwang, C.C., Edwards, J.C., 2005. The critical ventilation velocity in tunnel fires – a computer simulation. Fire Safety J. 40 (3), 213–244.

Kato, S., Murakami, S., Mochida, A., Akabayashi, S.I., Tominaga, Y., 1992. Velocity–pressure field of cross ventilation with open windows analyzed by wind tunnel and numerical simulation. J. Wind Eng. Ind. Aerod. 44 (1–3), 2575–2586.

Legion International Ltd., <http://www.legion.com/>.

Liu, P.C., Lin, H.T., Chou, J.H., 2009. Evaluation of buoyancy-driven ventilation in atrium buildings using computational fluid dynamics and reduced-scale air model. Build. Environ. 44 (9), 1970–1979.

Menter, F.R., 1994. Two-equation eddy-viscosity turbulence models for engineering applications. AIAA-J. 32, 1598–1605.

National Fire Protection Association, 1995. Handbook of Fire Protection Engineering, second Ed., NISTIR 4347 – SFPE.

National Research Council, 1991. Fires in Mass Transit Vehicles: Guidelines for the Evaluation of Toxic Hazards. Appendix D. Advisory Board: Commission on Engineering and Technical Systems, Transportation Research Board.

Papakonstantinou, K., Chaloulakoua, A., Ducia, A., Vlachakisb, N., Markatosa, N., 2003. Air quality in an underground garage: computational and experimental investigation of ventilation effectiveness. Energy Build. 35 (9), 933–940.

PIARC Committee on Road Tunnels, 1999. Fire and Smoke Control in Road Tunnels.

PIARC Technical Committee on Road Tunnel, 2004. Road Tunnels: Vehicle Emissions and Air Demand for Ventilation.

Raw, M.J., 1994. A coupled algebraic multigrid method for the 3D Navier Stokes equations. In: Proceedings of the 10th GAMM Seminar.

Raw, M.J., 1996. Robustness of coupled algebraic multigrid for the Navier–Stokes equations. In: Proceedings of the AIAA 34th Aerospace and Sciences Meeting & Exhibit, pp. 96–0297.

Rhie, C.M., Chow, W.L., 1982. A Numerical Study of the Turbulent Flow Past an Isolated Airfoil with Trailing Edge Separation. AIAA Paper 82, 0998.

Silva, M.C.G., Viegas, D.X., 1994. External Flow Field Around an Intercity Bus. In: Proceedings of the 2nd International Conference on Experimental Fluid Mechanics.

Stavrakakis, G.M., Koukou, M.K., Vrachopoulos, M.G., Markatos, N.C., 2008. Natural cross-ventilation in buildings: building-scale experiments, numerical simulation and thermal comfort evaluation. Energy Build. 40 (9), 1666–1681.

Still, G.K., 2000. Crowd Dynamics, Ph.D. Thesis, Warwick University, UK.

Tan, G., Glicksman, L.R., 2005. Application of integrating multi-zone model with CFD simulation to natural ventilation prediction. Energy Build. 37 (10), 1049–1057.

Van Maele, K., Merci, B., 2008. Application of RANS and LES field simulations to predict the critical ventilation velocity in longitudinally ventilated horizontal tunnels. Fire Safety J. 43 (8), 598–609.

Wong, N.H., Song, J., Istiadji, A.D., 2006. A study of the effectiveness of mechanical ventilation systems of a hawker center in Singapore using CFD simulations. Build. Environ. 41 (6), 726–733.

Yang, G.S., An, Y.L., Peng, L.M., Zhang, J.H., 2006. Simulation of smoke flow and longitudinal ventilation in tunnel fire. T. Nonferr. Metal. Soc. 16 (3), 741–746.

Yuan, F.D., You, S.J., 2007. CFD simulation and optimization of the ventilation for subway side-platform. Tunn. Undergr. Sp. Tech. 2 (4), 474–482.

Yuen, W.W., Tien, C.L., 1977. A simple calculation scheme for the luminous Flame emissivity. In: Proceedings of the 16th Symposium (International) on Combustion. The Combustion Institute, Pittsburgh, USA. pp. 1481–1487.

Zhou, Y., Wang, J., Huang, Di., Sun, S., 2010. Pedestrian simulation modeling for world expo 2010 Shanghai. J. Transport. Syst. Eng. Informat. Technol. 9 (2), 141–146.

Please cite this article in press as: Domingo, J., et al. Analysis and optimization of ventilation systems for an underground transport interchange building under regular and emergency scenarios. Tunnel. Underg. Space Technol. (2010), doi:10.1016/j.tust.2010.07.001